Proceedings of the International Conference "Underwater Acoustic Measurements: Technologies &Results"
Heraklion, Crete, Greece, 28th June – 1st July 2005

PASSIVE ACOUSTIC AND SEISMIC TOMOGRAPHY WITH OCEAN AMBIENT NOISE IN ORION

Peter Gerstoft, Karim Sabra, Philippe Roux, WA Kuperman, and William S Hodgkiss

Marine Physical Laboratory
Scripps Institution of Oceanography
University of California, San Diego

Abstract: *We demonstrate that an estimate of the point-to-point seismic propagation Green Functions can be extracted from microseisms. These estimated Green's function, obtained from 30 days of continuous seismic data from 151 seismic stations in Southern California, are used to extract the group velocity of surface waves between all station pairs in the network. The seismic data were then used in a simple, but densely sampled tomographic procedure to estimate the surface wave velocity structure within the frequency range of 0.1-0.2 Hz for a region in Southern California. The result compares favorably with previous estimates obtained using more conventional and elaborate inversion procedures. This demonstrates that coherent noise field between station pairs can be used for seismic imaging purposes.*

Keywords: *Orion, Noise crosscorrelation, Tomography, Green's function*

1. INTRODUCTION

We have demonstrated with ocean acoustic data and associated theory (Roux at 2004,2005) and land seismic data (Sabra et al, 2005a, 2005b) that the Green's functions between pairs of receiving sensors can be obtained from a long time correlation process. The ORION facility will provide an opportunity to study ocean and seismic structure and their time evolution with ambient noise. Noise data from fixed acoustic and seismic sensors can be used to study the ocean structure, the ocean bottom structure below the ORION sensor field and the earth structure between the Orion sensors and land sensors hundreds to thousands of

km away. We have already performed extensive seismic noise tomography using land sensors in Southern California (Sabra et al.; 2005a, 2005b) in which the major noise component originated in the ocean. We present the previous data analysis that demonstrates the feasibility of this concept as per exploiting the ORION concept. Further, we also describe the sensor characteristics necessary to collect invertible data.

Imaging the structure of the Earth traditionally uses the measured response from energetic active controlled sources (e.g. explosions or seismic vibrators) or specific earthquakes in order to infer part of the arrival-times of the local Time Domain Green's Function (TDGF). On the other hand, an estimate of the TDGF between pairs of seismic stations can be extracted from the coherent, deterministic arrival-times obtained from the time-derivative of the Noise Cross-correlation Function (NCF) (Rickett and Claerbout 1999; Weaver and Lobkis, 2001). This TDGF estimated from the noise field alone includes all tensor components of the Green's function. The resulting waveforms can be used to infer Earth structure from existing worldwide networks of broadband seismic stations, without relying on active sources or identifiable earthquakes.

Experimental and theoretical confirmation have shown that the arrival-time structure of the TDGF can be estimated from the NCF in various environments and frequency ranges of interest: helioseismology (Rickett and Claerbout 1999), ultrasonics (Weaver and Lobkis, 2001), ocean acoustics (Roux et al., 2004), and seismology (Shapiro and Campillo, 2004; Snieder, 2004; Wapenaar, 2004; Sabra et al., 2005b; Shapiro et al., 2005; Sabra et al., 2005c). The physical process underlying this noise cross-correlation technique is similar for all these environments. Initially, the small coherent component of the noise field at each receiver is buried in the spatially and temporally incoherent field produced by the distribution of noise sources. The coherent wavefronts emerge from a correlation process that accumulates contributions over time from noise sources whose propagation path passes through both receivers.

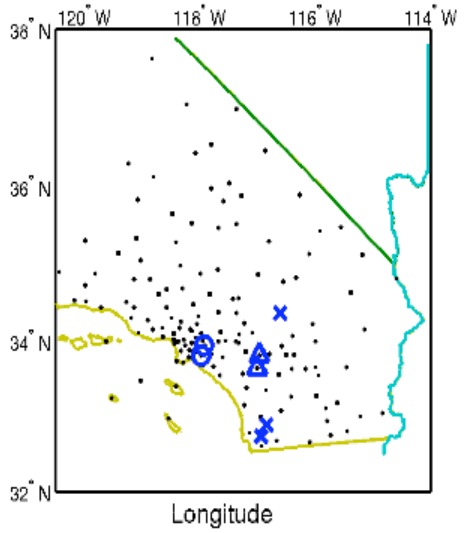

Figure 1 Map of the 150 online stations in the Southern California Seismic network, cross: JVA, SDG.

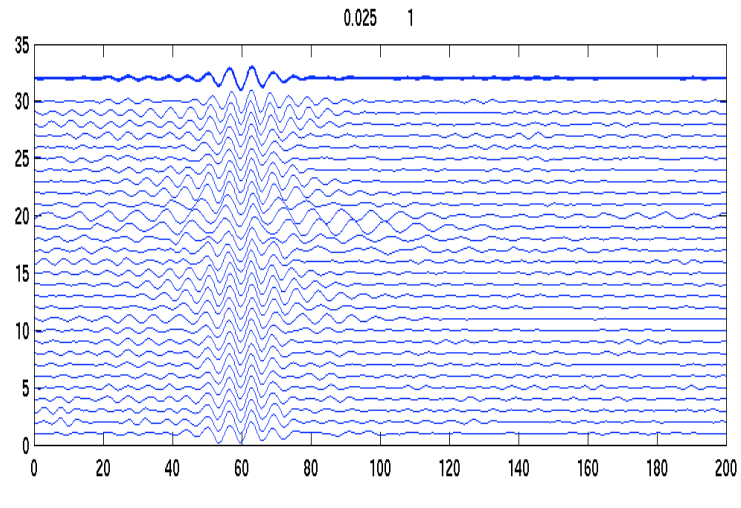

Figure 1 Bandpassed filtered 0.025-1 Hz cross correlation between stations JVA/SDR for each of 30 days of July using (top) full noise trace for each station and (bottom) single bit trace.

2. PROCESSING

For demonstrating the approach, data from the whole July 2004 for all seismic stations available from the Southern California Data Centre was used as indicated on Fig 1. All data was sampled at 1-Hz. The network contains 151 stations; cross correlating the observed time series for an entire month between all the stations gives potentially (151*150/2)= 11325 seismic traces. Thus, it is important that all the processing is automatic and efficient.

In order to estimate the NCF, the noise traces are first band pass filtered. Next, we note that this cross-correlation technique works best when the noise distribution is uniform in space and time (Larose et al 2004; Snieder, 2004; Shapiro and Campillo, 2004; Roux et al., 2004). Hence the effects of large seismic events should be minimized since they would otherwise dominate the arrival-time structure of the NCF. Clipping all signals above a certain threshold reduces these events. The clipping threshold is determined as the minimum of the standard deviations measured over each day, expecting that few events appear in that time interval, and the threshold is only determined by the noise. This way the effect of large events is reduced, but the high frequency content of the seismic noise spectrum is less distorted. For each entire day in July 2004 the processing is carried out for station pair SDG/JVA for 0.05-0.5 Hz pass band as shown in Fig 2. An arrival is very clearly seen centred at t=60 s.

3. EXTRACTING RECORD SECTIONS

The above crosscorrelation of the vertical noise components was applied to all 151 station-pairs in the Southern California network using a 0.1-0.2 Hz passband and averaging over all days in July. All station pairs were oriented so that the pointed from East to West. Figure 4 shows a "record section" from this processing based on the envelope of the NCF derivative. For the station pairs pointing away from the ocean (Fig 4 left) a clear that the recovered signals are propagating wavetrains with an average group velocity of 2.8 km/s. Most of the noise originates from microseisms and therefore the time series for station pairs perpendicular to the coast emphasize the forward propagating Greens function. For the station pairs parallel to coast (Fig 4 right) two wavestrains propagating in both the forward and backwards direction with an average group velocity of 2.8 km/s.

For the station pairs parallel to the coast there is no prominent propagation direction and waves are propagating in both the forward and backward direction, and are much more noisy (as discussed below). Scattering from heterogeneities and geometric effects (e.g. such as reflections from the edge of a basin randomize the noise field and thus partially redistribute the ocean microseisms arrival direction more uniformly. Some station pairs oriented parallel to the coast have a clear waveform and this may be due to scattered ocean noise propagating along their station axis. However, the NCF for station pairs oriented perpendicular to the coast emerge overall more reliably and have sharper waveforms than for station pairs oriented parallel to the coast.

We estimated the group velocity of Rayleigh waves within the region containing the stations used in calculating the NCF record section by extracting an average layered P and S wave velocity model for the region from the 3D model of Kohler et al. (2003). Group velocity as a function of period was calculated for the model structure. The estimated group

velocity ranges from 2.8 km/s at 5-s period to 3.0 km/s at 10-s period, which agrees well with the estimated group velocity of 2.8 km/s at a period of about 6 s from our NCF record section.

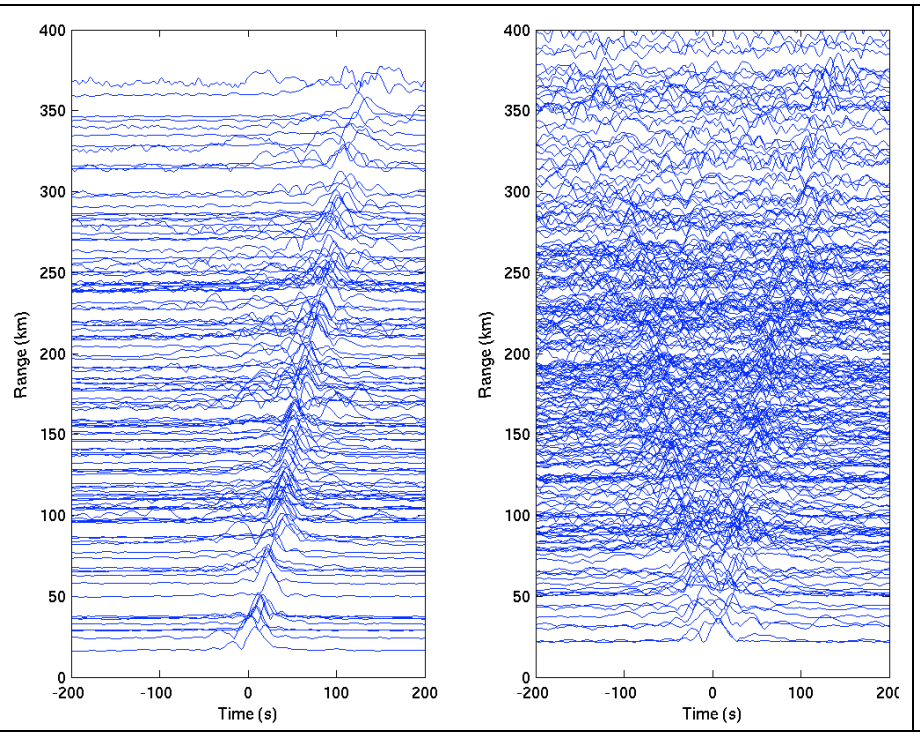

Figure 2 Envelope of the derivative of the NCF for all station paths with a distance less than 400 km Station pairs having a bearing between 18—20 (left), and 130-132 (right) deg to N for vertical component bandpass filtered at 0.1-0.2 Hz. Each trace has been normalized to the same amplitude.

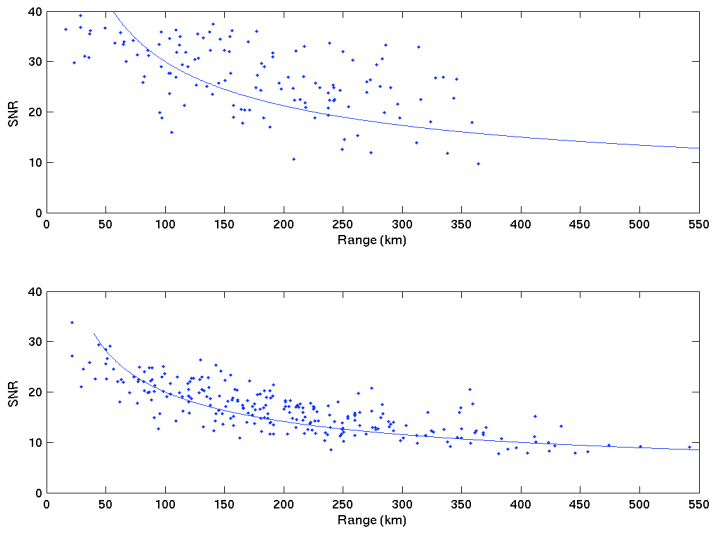

Figure 3 SNR versus range for each seismic trace in Fig XX, a) Station pairs having a bearing between (top) 18—20, and (bottom) 130-132 deg to N.

An important issue is the rate at which the waveforms emerge as a function of averaging time and separation distance (range). We define the SNR as the ratio (in dB) of the peak in a 50-s time-window centred around the main arrival r/c, c=2.8 km/s and the standard deviation for a noise-only time-window, -400 to -350 s. For the two record sections in Fig. 4 we see that the corresponding SNR in Fig. 4 is much lower (about 10 dB) for the station pairs perpendicular to the coast, thus there is clearly an azimuthally dependence. For the range dependence of SNR, intuitively and to first order, we expect the SNR to be proportional to $1/\sqrt{R}$ (dotted line) and this seems to hold reasonably well.

4. TOMOGRAPHY USING VERTICAL COMPONENT GREEN'S FUNCTION

The Southern California region is divided into 13 x 16 km constant group velocity cells for the tomographic inversion. The propagations paths are assumed to be straight rays. A simple the linear inversion method to construct the tomographic map is used. An example of an extracted surface velocity map is shown in Fig 5 (left). This map produces a residual variance reduction of 50% relative to residuals for the homogenous model. There is a good correlation between the group velocity obtained from the surface wave inversion map (Fig 5 left) and several geological features of the Southern California (Shapiro et al., 2005). Slow surface wave velocity regions (labels A-D) correspond to sedimentary basins. Fast group velocities characterize mountain ranges (labels E (Peninsular Ranges) and F (Sierra Nevada)). The main imaged geologic units are consistent with Shapiro et al. (2005). However a greater velocity contrast is observed 1) along the San Andreas Fault and 2) on the East of the Great Basin and the Mojave Desert, along a low velocity zone extending approximately from (117W,36N) to (116W,33.5N).

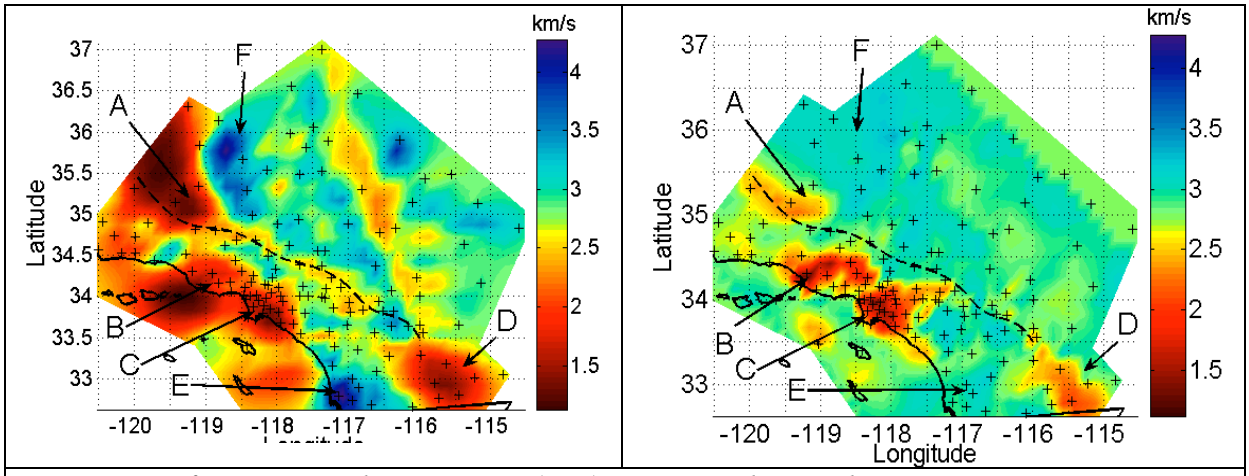

Figure 4 Surface group velocity maps. (Top) corresponding to the maximum a posteriori solution for the tomographic inversion scheme. Low resolution area (determined from Fig. 12) were masked. (Bottom): Estimated map of the 0.1-0.2 Hz Rayleigh wave group velocity of the Earth's crust (see Eq. 5) constructed from a 3D velocity model for the Southern California region. (A: San Joaquin valley, B: Ventura, C: Los Angeles, D: Salton Sea Trough) .

This tomographic map also agrees quantitatively with an estimated group velocity map derived from previous 3D models (Kohler *et al., 2003*) (Fig 5 right). The Rayleigh wave velocity was estimated as 0.91 times the value of the average shear wave velocity of the shallow Earth crust for an exponentially decaying Rayleigh wave over depth. Hence, the estimated Rayleigh wave group velocity C_R in Fig 5 right is defined by averaging the variation of the shear velocity obtained from *Kohler et al., (2003)* $c_s(z)$ over depth z:

$$C_R = 0.91 \int_0^Z c_s(z) \exp(-kz) dz \Big/ \int_0^Z \exp(-kz) dz , \qquad (6)$$

where Z=8km, $k=2\pi f/c_0$, and f=0.15Hz (average center frequency).

CONCLUSION

Estimates of the surface wave components of the time domain Greens function (TDGF) can be extracted from the time-derivative of the noise cross-correlation between two stations. Broadband noise cross-correlations computed over a dense network of station pairs exhibit frequency dispersion and three-dimensional variations of the arrival-time structure. Short-period content is more likely to be recovered for short propagation distances. These waveforms can be used as a basis for constructing a geophysical model. The observed emergence of the coherent waveforms confirms that they build up proportional to the square root of the recording time.

The TDGF was estimated from crosscorrelation of continuous noise recordings dominated by ocean microseisms in the frequency band [0.1-0.2 Hz]. A high-resolution tomographic map for surface wave group velocity in Southern California was constructed using the estimated TDGF with signal-to-noise ratios larger than 10-15 dB.

Acknowledgments: Funding was provided by the UCSD/LANL CARE-program and the Office of Naval Research. Data came from the Southern California Earthquake Center.

REFERENCES

1. Kohler, M.D., H. Magistrale, and R.W. Clayton, 2003, Mantle Heterogeneities and the SCEC Reference Three-Dimensional Seismic Velocity Model Version 3, Bull. Seism. Soc. Am., **93**, 757-774.
2. Larose E., A. Derode, M. Campillo and M. Fink, 2004, Imaging from one-bit correlations of wideband diffuse wavefields, J. Appl. Phys., **95**, 8393-8399.
3. Rickett, J. and J. Claerbout, 1999, Acoustic daylight imaging via spectral factorization: Helioseismology and reservoir monitoring, The Leading Edge, **18**, 957-960.
4. Roux, P., W.A. Kuperman, and the NPAL Group, 2004, Extracting coherent wavefronts from acoustic ambient noise in the ocean, J. Acoust. Soc. Am., **116**, 1995—2003.
5. Roux, P., K.G. Sabra, W.A. Kuperman and A. Roux, 2005, Ambient noise cross-correlation in free space: theoretical approach, J. Acoust. Soc. Am., **117**, 79—84.
6. Sabra, K.G., P. Gerstoft, P. Roux, W.A. Kuperman and M. C. Fehler (2005a), Extracting time-domain Greens function estimates from ambient seismic noise, Geophys. Res. Lett., **32**, doi:10.1029/2004GL021862.
7. Sabra, K.G., P. Gerstoft, P. Roux, W.A. Kuperman, and M.C. Fehler, 2005b, Surface wave tomography from microseisms in Southern California, submitted AGU Geophysical Research Letters.
8. Shapiro, N.M. and M. Campillo, 2004, Emergence of broadband Rayleigh waves from correlations of the ambient seismic noise, Geophys. Res. Lett., **31,** L07614.
9. Shapiro, N.M., M. Campillo, L. Stehly and M.H. Ritzwoller, 2005, High-resolution surface wave tomography from ambient seismic noise, Science, **307**, 1615-1617.
10. Snieder, R., 2004, Extracting the Green s function from the correlation of coda waves: A derivation based on stationary phase, Physical Review E, **69**, 046610.
11. Wapenaar, K., 2004, Retrieving the Elastodynamic Green's Function of an Arbitrary Inhomogeneous Medium by Cross Correlation, Phys. Rev. Lett., **9**3, 254301.
12. Weaver, R.L., and O.I. Lobkis, 2001, Ultrasonics without a Source: Thermal Fluctuation Correlations at MHz Frequencies, Phys. Rev. Lett., **87**, 134301.